

DOI: <http://dx.doi.org/10.21123/bsj.2022.19.2.0347>

Protection of Galvanized steel from corrosion in salt media using sulfur nanoparticles

*Rasha A. Jassim**

Muna S. Sando

Ahlam M. Farhan

Department of Chemistry, College of Science for Woman, University of Baghdad, Baghdad, Iraq.

*Corresponding author: rshaabd3165@gmail.com, munasando1971@gmail.com, af8832@gmail.com

*ORCID ID: <https://orcid.org/0000-0003-3827-3306>, <https://orcid.org/0000-0001-7432-7944>, <https://orcid.org/0000-0002-7700-5657>

Received 13/6/2020, Accepted 3/11/2020, Published Online First 20/9/2021, Published 1/4/2022



This work is licensed under a [Creative Commons Attribution 4.0 International License](https://creativecommons.org/licenses/by/4.0/).

Abstract:

The characteristics of sulfur nanoparticles were studied by using atomic force microscope (AFM) analysis. The atomic force microscope (AFM) measurements showed that the average size of sulfur nanoparticles synthesized using thiosulfate sodium solution through the extract of cucurbita pepo extra was 93.62 nm. Protecting galvanized steel from corrosion in salt media was achieved by using sulfur nanoparticles in different temperatures. The obtained data of thermodynamic in the presence of sulfur nanoparticles referred to high value as compares to counterpart in the absence of sulfur nanoparticles, the high inhibition efficiency (%IE) and corrosion resistance were at high temperature, the corrosion rate or weight loss decreased with increasing temperature in the presence of sulfur nanoparticles. The positive value of enthalpy ΔH^* for galvanized steel with and without sulfur nanoparticles indicates that the reaction was endothermic. Therefore, the sulfur nanoparticles can be suggested as good inhibitor for galvanization in salt media.

Key words: Cucurbita pepo extra, Corrosion, Galvanized steel, Sulfur nanoparticles, Thermodynamic parameters, Thiosulfate sodium.

Introduction:

The small size and high ratio of surface to volume of nanoparticles have novel characteristics compared with bulk material¹. The shape and size of nanoparticles depend on many properties, such as applications ranging from catalysts, transistors of computer, activity of antimicrobial, sensors of chemical and electrometers. The nanoparticles were used in many fields for example nanocomposites, drug, medical and hyperthermia². The sulfur nanoparticles were used in diseases of plant for example scab of apple, grapes culture, strawberry and vegetables. In agriculture, sulfur nanoparticles were used due to good efficiency pesticide also black spot and powdery mildew diseases. The sulfur nanoparticles have high quantum size properties and surface area³. They are also used in animals and humans diseases such as dandruff causing malassezia furfur. There are many techniques for the synthesis of sulfur nanoparticles such as hydrolysis methods by using sodium polysulphide, precipitation technique for unique membrane-

assisted also liquid phase and microemulsion method for water –oil, these techniques involve physical and chemical approaches⁴. Using galvanized steel compared with other materials due to that galvanized steel has good strength, formability and production economics. The reason why steel is the preferred material is because of its resilience, strong, recyclable and economical form. The steel forms stable bonds of iron and oxide salts because it interacts with substances in the atmosphere, and these reactions depend on the concentration of the substances and the nature of the corrosive substances present in the environment. The steel is protected from corrosion by using the galvanizing method, and this method is the most used, as the use of the galvanizing method reduces the replacement of the metal and thus saves energy⁵. Because galvanized steel is resistant to corrosion, it is therefore used in many magazines, including under sea water, car parts, and others. Due to the zinc coating, the metal is rust-resistant, but when

the zinc surface is wet with rain, an electrochemical process begins, causing atmospheric corrosion of the galvanized steel structure⁶. Cucurbitaceous is family of cucurbita pepoL, cucurbita pepo L which consist of fatty acids, vitamins E, phytosterol, flavonoids and mineral rich of zinc. The best time to sowing cucurbita pepoL in spring is when temperature is 15°C and the sowing is at depth 10 cm⁷. Summer squash (*Cucurbita pepo* L.) is an annual vegetable crop which belongs to Cucurbitaceous family. It is the main source of carbohydrates, dietary fibers, minerals (Ca, Mg, P and Zn) and many important vitamins⁸. The sea water corrosivity depends on multiple factors⁵, such as: salinity, dissolved oxygen, temperature, different types of biological factors⁶ (bacteria, fungus, algae), relative displacement of corrosion medium, exposed type of metal. The type of corrosion depends on the mineral exposed to the influence of sea water, so marine corrosion is known as electrochemical corrosion, i.e. an oxidation process (anodizing) and a reduction process (cathodic). This corrosion is wet erosion and has many effects, as the metal is classified in a specific order, known as the galvanic chain, because the corrosion is bimetallic⁹.

Materials and Methods:

2.1- Material

The galvanized steel which has been used in the work had the following composition shown in Table 1¹⁰.

Table 1. The chemical composition of the base metal (carbon steel) .

Metal	Co	Si	Mn	S	P
Wt%	0.40	0.25	0.80	0.015	0.015

When the carbon steel coated with zinc by using hot-dip process with thickness equal 0.080 nm, then the chemical composition of zinc layer becomes as shown in Table 2.

Table 2. The chemical composition of the zinc layer.

Metal	Zn	Al	Sn
Wt%	99	0.5	0.5

2.2-Preparation of metal

The galvanized steel was treated by emery paper of different grades from 300 to 1200 up grit ,this process gave smooth surface of metal then washed with Ion-free water, then an ultrasound device is used to clean the metal with acetone, and then it is dried with warm air.

2.3- Preparation of Test Solution

The test solution (3.5% NaCl) is prepared by dissolving 35 g NaCl in 1 L distilled water.

2.4- Preparation of Cucurbita pepo leaf extra

The first step in this work was wishing the leaves with tap water then deionized water and dried at room temperature. The leaves were cut into small pieces, after that 20g of Cucurbita pepo leaf was added to 100ml deionized water and boiled for 1 h at 100°C. The mixture was departed by using centrifuge for 30 min., the solute was kept to use.

2.5-Preperation of sulfur nanoparticles

The mixture of 20ml of Cucurbita pepo leaf extra with 50ml sodium thiosulfate pentahydrate, was stirred for 10min. Then 25 ml of 20% citric acid was added with keeping stir for 30 min. The formation precipitation was collated and kept until use¹¹.

2.6- Potentiodynamic polarization measurements

The measurements of electrochemical parameter were used potentiostatic Set –Up, which consisted of the thermostat, host computer, magnetic stirrer and M lab potentiostat- galvanostat. The medium was 3.5%NaCl solution at different temperatures. Corrosion cell have three electrodes (name of electrodes), in the working electrode paced galvanized steel holder with caver opening size 1cm, counter electrode was Pt wire and the reference electrode, that consisted of silver-silver chloride placed near surface working electrode, the test solution was filled in the reference electrode. The open circuit potential (Ecor) was calculated from steady state potential then recorded the cathodic direction of potential and the anodic direction. Fig. 1 shows potentiostatic Set –Up.

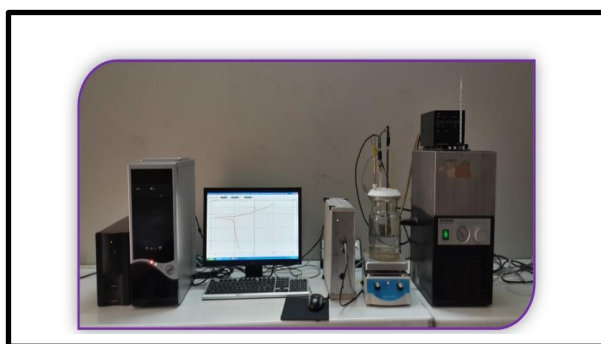


Figure 1. Potentiostatic Set –Up

Results and Discussion:

3.1-Atomic Force Microscope (AFM) measurements

The technique AFM was scanning microscope probe, the major task of Atomic Force Microscope is to account the force between the sample and tip. Force of repulsive between sample and tip was the basic idea. Atomic Force Microscope explained the

scan of the surface sample for image rebuilding from lines acquiring successive sulfur nanoparticles¹². Fig.2 shows all of AFM images of the sulfur nanoparticles, when the size was 93.62 nm, also the topography displayed adhesion force and peak

current. The recognition of surface materials by image area of different properties, is shown in Fig3. The particle size distribution and the average particles size around 93.62 nm.¹³

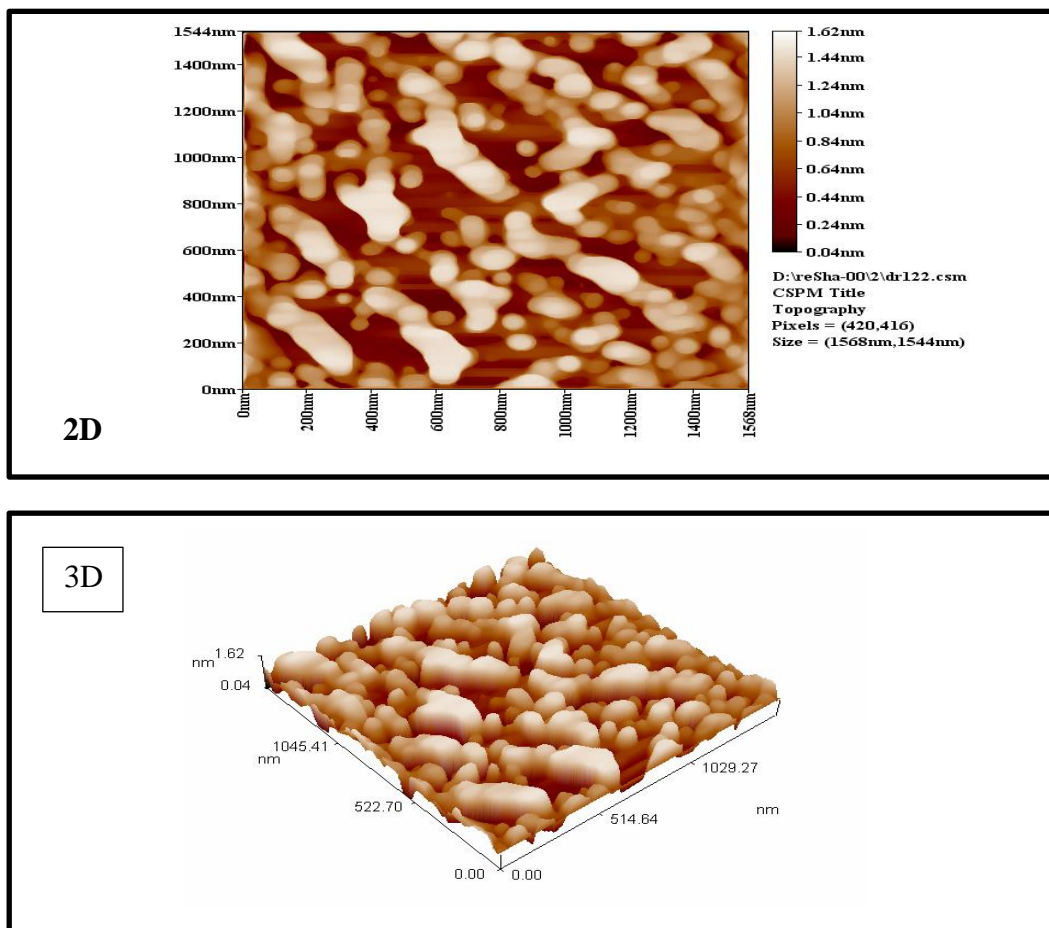


Figure 2. AFM images of the sulfur nanoparticles

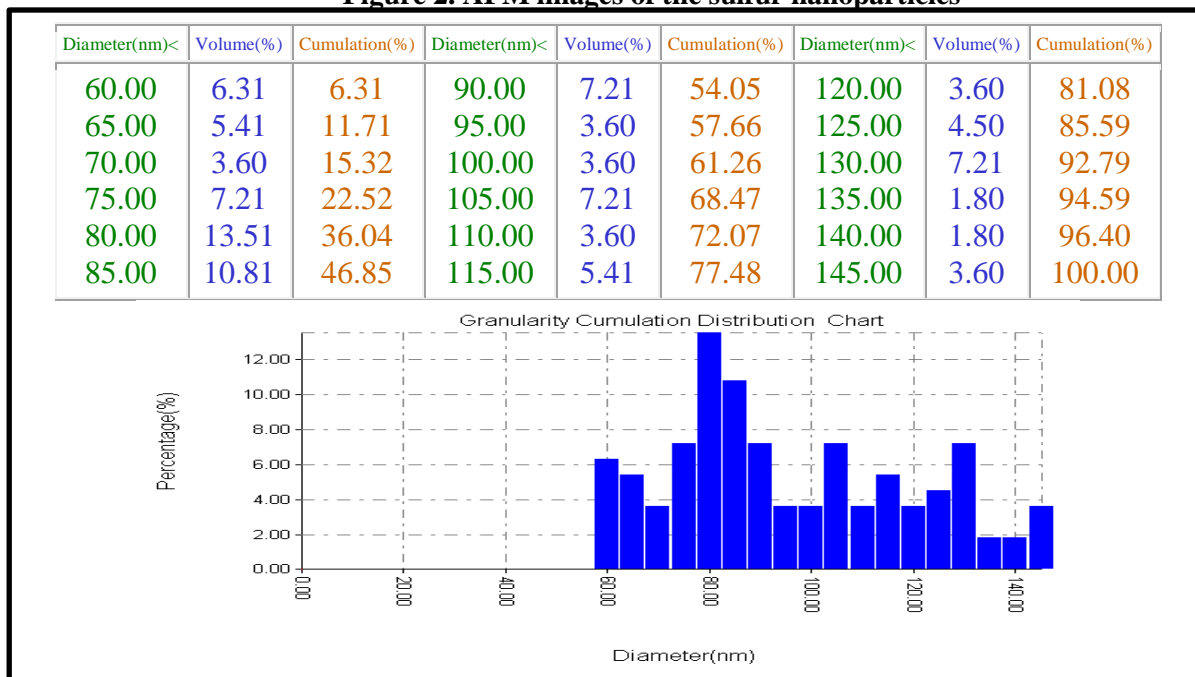


Figure 3. Granularity Cumulation Distribution Report

3.2-Potentiodynamic polarization

The explained polarization curves of galvanized steel with sulfur nanoparticles and without sulfur nanoparticles in salt media at different temperatures are shown in Figs. (4 and 5). Table 3 shows corrosion current density (I_{corr}), corrosion potential (E_{corr}), anodic Tafel line (ba), cathodic Tafel line (bc), inhibition efficiency (IE) and surface coverage (θ) for galvanized steel with and without sulfur nanoparticles in salt media at different temperatures (298, 308, 318 and 328). It has been found that increasing the temperature in the presence and absence of sulfur nanoparticles

caused shifting of the tafel lines to negative potential for anodic processes and positive potential for cathodic processes, due to that sulfur nanoparticles effectiveness on processes, Table 3 and Figs. (4 and 5) show the results. When applying external current, it has been obtained that when anodic was more polarized, then sulfur nanoparticles were anodic inhibitors. The values E_{corr} was more positive and (I_{corr}) decreased with increasing the temperature. This is attributed to the presence of sulfur nanoparticles, which induce an adsorption on surface galvanized steel¹⁴.

Table 3. Corrosion parameters of galvanized steel in presence and absence of nanoparticles in NaCl at four temperature (298, 308, 318 and 328) K.

galvanized steel absence sulfur nanoparticles	T (K)	$I_{(cor)}$ $\mu A/cm^2$	-E (corr) mV	-ba mV/Dec	bc mV/Dec	W.L or C.R (g/m ² .d)	P.L (mm/a)	IE%	θ	Rp/ $\Omega.cm^2$
galvanized steel absence sulfur nanoparticles	298	19.00	228.1	130.6	119.6	4.75E+000	2.21E-001	-	-	1426
	308	36.60	213.1	217.9	128.6	9.09E+001	4.22E-001	-	-	959.4
	318	40.95	206.9	156.5	106.3	1.02E+001	4.72E-001	-	-	671.23
	328	76.41	215.5	177.3	110.6	1.90E+001	8.80E-000	-	-	387.0
galvanized steel with presence sulfur nanoparticles	298	8.68	193.1	119.8	72.0	2.16E+000	1.00E-001	54.31	0.5431	2259.15
	308	9.07	181.8	106.8	88.4	2.28E+000	1.06E-001	75.21	0.7521	2315.48
	318	9.91	159.8	175.7	202.9	2.45E+000	1.14E-001	75.79	0.7579	4125.7
	328	12.18	218.5	185.6	203.4	2.55E+000	1.19E-001	84.05	0.8405	6114.8

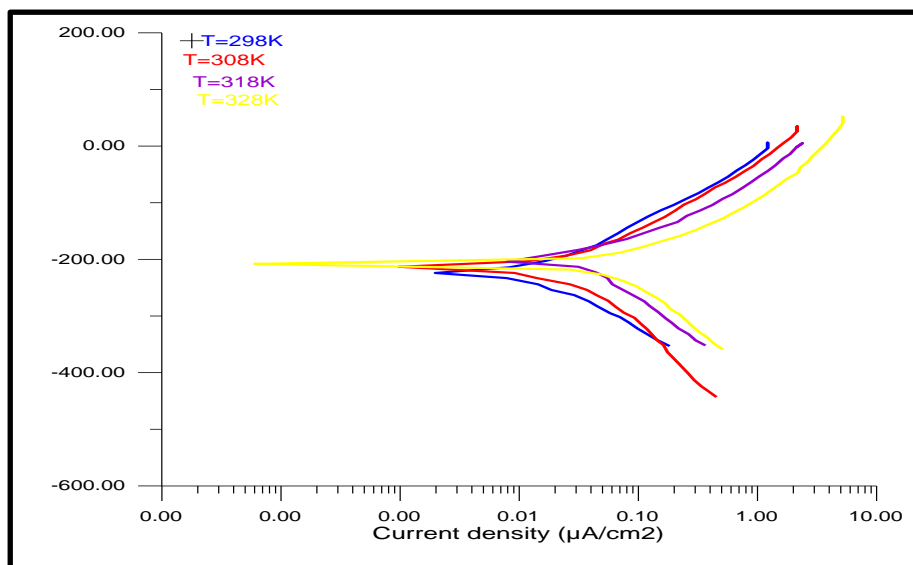


Figure 4. The polarization curves of Galvanized steel in sea water (3.5%NaCl) at different temperatures.

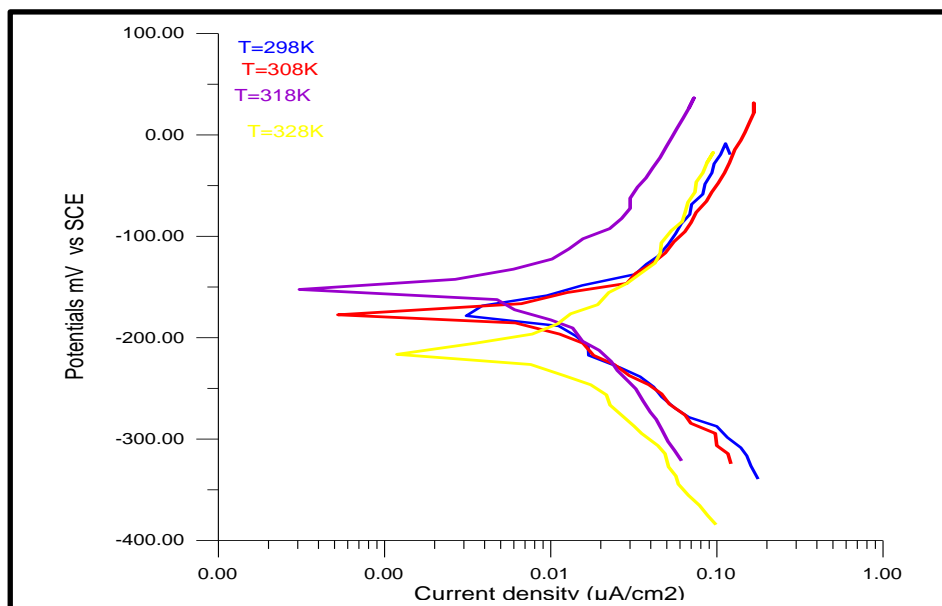


Figure 5. The polarization curves of Galvanized steel/ sulfur nanoparticles in sea water (3.5%NaCl) at different temperatures.

The protection efficiency (IE%) and surface coverage(θ) calculated from equation (1 and 2) ¹⁵.

$$IE \% = (I_0 - I) / I_0 \times 100 \dots \dots \dots 1$$

$$\theta = (I_0 - I) / I_0 \dots \dots \dots 2$$

Where, IE% = inhibition efficiency, I_0 and I are the corrosion current density without and with the inhibitor respectively. Table 3 shows the results of increasing temperature, increasing protection efficiency and surface coverage due the sulfur nanoparticles adsorption on surface galvanic steel in salt media at different temperature. It can be noticed that the tafel lines shifted to more positive potential and more negative potential during cathodic processes and anodic processes ¹⁶.

The resistors polarization (R_p) was increasing with the presence of sulfur nanoparticles therefore the sulfur nanoparticles can be a good inhibitor for galvanized in salt media ¹⁷.

3.3-Thermodynamic study

The data listed in Table 4 will be used as reference to evaluate the thermodynamic parameter for corrosion galvanized steel in absence and presence

of sulfur nanoparticles in salt media at different temperature.

3.3.1-The activation energy

The data listed in Table 4 will be used as a reference to evaluate the thermodynamic parameter for corrosion galvanized steel in the absence and presence of sulfur nanoparticles in salt media at different temperature.

3.3.1-The activation energy

The activation energy was estimated from equation 3 ¹⁸.

$$\log CR = - \frac{E_a}{2.303RT} + \log A \dots \dots \dots 3$$

Where (C_R) The corrosion rate, T is absolute temperature (K), R is constant of universal gas (8.314 J/mol K) and A is the Arrhenius pre-exponential constant. According to the equation 3, plots of $\log C_R$ versus $1/T$, the slope of the straight line is equal to the activation energy and intercept with the presence of sulfur nanoparticles (part 7) show the increase of increasing the activation energy in the presence of sulfur nanoparticles comparing with the results in the absence of sulfur nanoparticles due to forming thin film on the surface of metal, the metal increased energy barrier. Therefore the adsorption of sulfur nanoparticles on surface of galvanic steel was physical adsorption.

Table 4. Values of thermodynamic functions with presence and absence for galvanized steel of sulfur nanoparticles at different temperatures in 3.5% NaCl .

galvanized steel absence sulfur nanoparticles	T(K)	$\Delta G/$ KJ/mol	$E_a/$ KJ/mol	A Molecules. $\text{cm}^{-2} \cdot \text{S}$	$\Delta H/$ KJ/mol	$-\Delta S/$ J/mol
	298	65.618	35.2020	4.656×10^{19}	32.615	110.7594
	308	66.726				
	318	67.833				
	328	68.941				
galvanized steel presence sulfur nanoparticles	T(K)	$\Delta G/$ KJ/mol	$E_a/$ KJ/mol	A Molecules. $\text{cm}^{-2} \cdot \text{S}$	$\Delta H/$ KJ/mol	$-\Delta S/$ J/mol
	298	67.741	90.59	15.645×10^{19}	6.4432	205.7022
	308	69.79				
	318	71.855				
	328	73.912				

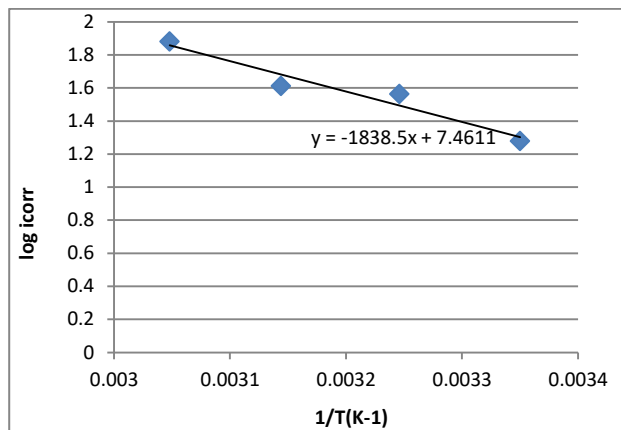


Figure 6. Plot of log icorr against 1/T for Galvanized steel in 3.5% NaCl in the absence of sulfur nanoparticles at different temperatures.

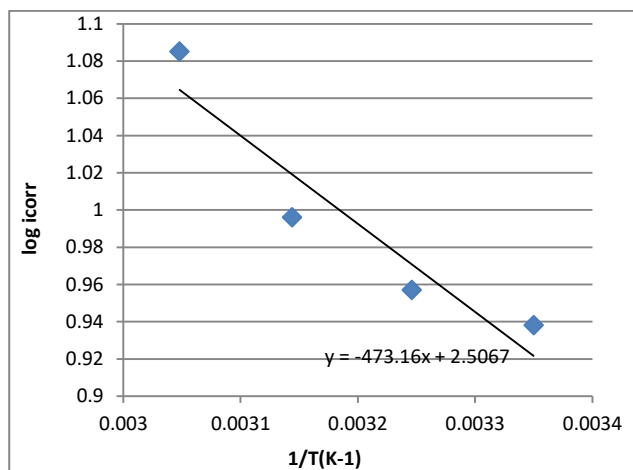


Figure 7. plot of log icorr against 1/T for Galvanized steel in 3.5% NaCl in the presence of sulfur nanoparticles at different temperatures.

3.3.2-Enthalpy and Entropy

Enthalpy and entropy functions can be calculated from equation 4¹⁹.

$$\log(\text{icorr}/T) = \log(R/Nh) + \frac{\Delta S}{2.303R} - \frac{\Delta H}{2.303R} \dots \dots \dots 4$$

Where h is the Plank constant, N is Avogadro number, R is the constant of universal

gas (8.314 J/mol K), ΔH is the enthalpy activation and ΔS is the entropy activation. Figs.(8 and 9) show a plot of $\ln (\text{icorr}/T)$ against $1/T$ for the galvanized steel only and galvanized steel with sulfur nanoparticles. Straight lines are obtained with a slope of $(-\Delta H /R)$ and an intercept of $(\ln R/Nh + \Delta S /R)$ from which the values of ΔH and ΔS are calculated and listed in Table 4¹⁹. Analysis of the values listed in Table 4 show that the positive values of the activation enthalpy ($+\Delta H$) of the dissolution reaction of galvanized steel in 3.5% NaCl in the presence of the sulfur nanoparticles are greater compared to the case of the free. The positive sign of these enthalpies reflect the endothermic nature of the galvanized steel dissolution process, because decreasing the corrosion rate of galvanized steel was controlled by the activation of kinetic parameters also the value of activation energy was larger than the value enthalpy²⁰. The value of entropy was positive value, this is indicates that the complexity in the rate determination steps was activated rather than dissociation steps, the activated complexity became more associated in the rate determination when the inhibitor was in a higher concentration²¹.

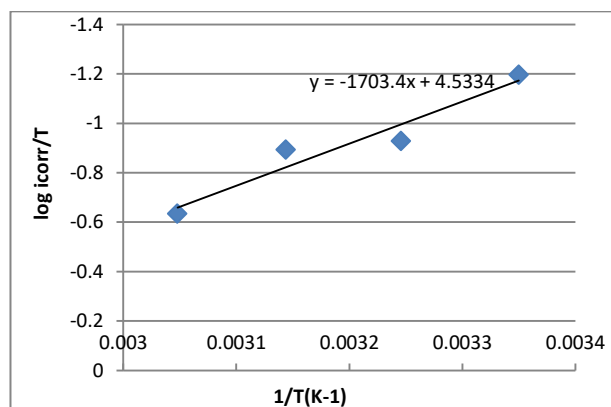


Figure 8. plot of log (icorr/T) against 1/T for Galvanized steel in 3.5% NaCl in the absence of sulfur nanoparticles at different temperatures.

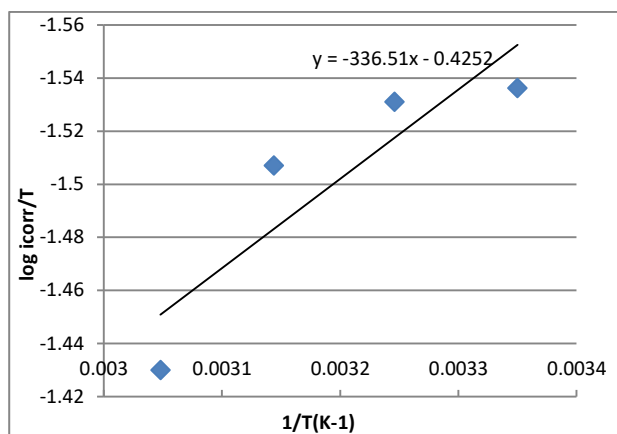
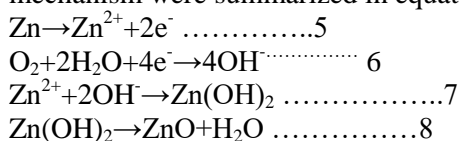


Figure 9. plot of $\log(icorr/T)$ against $1/T$ for Galvanized steel in 3.5% NaCl in the presence of sulfur nanoparticles at different temperatures.

3.4-Mechanism of corrosion

The chemical reaction steps of corrosion mechanism were summarized in equation 5-9²².



Than Cl^- contact to ZnO to formation $\text{Zn}_5(\text{OH})_8\text{Cl}_2 \cdot \text{H}_2\text{O}$.



The compound $\text{Zn}_5(\text{OH})_8\text{Cl}_2 \cdot \text{H}_2\text{O}$ is less corrosion and repel aggressive ions.

Authors' declaration:

- Conflicts of Interest: None.
- We hereby confirm that all the Figures and Tables in the manuscript are mine ours. Besides, the Figures and images, which are not mine ours, have been given the permission for republication attached with the manuscript.
- Ethical Clearance: The project was approved by the local ethical committee in University of Baghdad.

Authors' contributions statement:

- Title of manuscript: Protection of Galvanized steel from corrosion in salt media using sulfur nanoparticles
- The authorship of the title above certify that they have participated in different roles as follows:
- Rasha A. Jassim: Preparation, Analysis, Curation of data, Study, Writing –main draft.
- Ahlam M. Farhan: Conceptualization, analysis, Resources, Visualization, Editing Writing.
- Muna S. Sando: Analysis, Curation of data, Study, Writing.
- The Final Paper was read and authorized by all Writers.

References:

1. Mohd SA, Jitendra P, Yeoung SY. Biogenic Synthesis of Metallic Nanoparticles by Plant Extracts. ACS Sustainable Chem. Eng. 2013; 1: 591–602.
2. Siavash I. Green synthesis of metal nanoparticles using plants. Green Chem. 2011; 13: 2638–2650.
3. Nidá M S, Luma SA, Akl MA, Qusay MI, Amany OA. Green Synthesis of Nano-Sized Sulfur and Its Effect on Plant Growth. AS Journal. 2016; 8(1):188-194.
4. Priti P, Mahendra R. Bio-inspired synthesis of sulphur nanoparticles using leaf extract of four medicinal plants with special reference to their antibacterial activity. IET Nanobiotechnol. 2018; 12(1): 25 – 31.
5. Abdel Hamid ZS, Abd El Rehim S, Ebrahim MA. Improvement the Corrosion Resistance for the Galvanized Steel by Adding Sn. JSEMAT. 2016; 6: 58-71.
6. Merajul MH, Alam SL, Moniruzzaman M, Mohar AB. Corrosion comparison of galvanized steel and aluminum in aqueous environments. IJAME. 2014;9:1758-1767.
7. Latifi, M, Barimavandi A, Sedaghatoor S, Lipayi SR. Sowing Date and Plant Population Effects on Seed Yield of Cucurbita pepo. Int. J. Agric. Biol. 2012; 14(4): 641–644.
8. Pankaj KK, Ram A, Awani KS, Eldho V. Postharvest treatments to reduce chilling injury in summer squash (Cucurbita pepo) fruits during storage. Indian J Agr Sci. 2019; 89 (10): 1633–7.
9. Nejneru C, Savin C, Perju M C, Burduhos N D, Costea M, Bejinariu C. Studies on galvanic corrosion of metallic materials in marine Medium. IOP Conf. Ser.: Mater. Sci. Eng. 2019; 10: 1-8.
10. Hayfaa A A. Corrosion and Corrosion Inhibition Study of Galvanized Steel in Salty Acidic and Basic Media. Ministry of Higher Education and Scientific Research, University of Baghdad, College of Pharmacy. 2012.
11. Tripathi RM., Pragadeeshwara RR, Takuya T. Green synthesis of sulfur nanoparticles and evaluation of their catalytic detoxification of hexavalent chromium in water. RSC Adv. 2018; 8: 36345–36352.
12. Chicea D, Indrea E, Cretu C M. Assessing Fe₃O₄ nanoparticle size by DLS, XRD and AFM. JOAM. 2012;14(5- 6): 460 – 466.
13. Renate H, Seniz S, Rémi C, Linus C, Ines G, Natalia C, Brigitta P, Andreas K F. AFM as an analysis tool for high-capacity sulfur cathodes for Li–S batteries. Beilstein J. Nanotechnol. 2013; 4: 611–624.
14. Badiea A. M., Hani A D, Abdulghani A. S., Kikkeri N M. Inhibition of Low Carbon Steel Pipes of Heat Exchangers in Industrial Water Medium by Some Plants Extract. J. Mater. Environ. Sci. 2013; 4 (3):390-403.
15. Abdulasoul Salih Mahdi. Amoxicillin As Green Corrosion Inhibitor for Concrete Reinforced Steel In Simulated Concrete Pore Solution Containing Chloride. Ijaret. 2014; 5(6): 99-107.
16. Ayman MA, Hamad AA, Gamal AE, Abdel ROE. Application of Stabilized Silver Nanoparticles as Thin Films as Corrosion Inhibitors for Carbon Steel

- Alloy in 1M Hydrochloric Acid, Hindawi Publishing Corporation. JNM. 2013; 10 :1-8.
17. Noor AK, Abdulkareem MA. Role of Carbon Dioxide on the Corrosion of Carbon Steel Reinforcing Bar in Simulating Concrete Electrolyte. Baghdad Sci. J.2020; 17(1):93-98.
18. Olatunde AA , Oludare JO, Ebenezer LO .Thermodynamics and adsorption study of the corrosion inhibition of mild steel by Euphorbia heterophylla L. extract in 1.5 M HCl, Results in Materials.2020; 5 :1-7.
19. Batah A, Anejjar A, Belkhaouda M, Bammou L, Salghi R, Bazzi L, Hammouti B, chetouani A. Electrochemical and thermodynamic study of the inhibitory efficacy of Methanol extracts of the Rind and Leaves of Grapefruit plant on the corrosion of carbon steel in an acidic medium. Mor. J. Chem.2017; 5 (3): 404-416.
20. Hamdy A, Nour SG. Thermodynamic, adsorption and electrochemical studies for corrosion inhibition of carbon steel by henna extract in acid medium, Egypt. J Pet., 2013; 22: 17–25.
21. Norzila M, Anis S I. Thermodynamic Study of Corrosion Inhibition of Mild Steel in Corrosive Medium by Piper nigrum Extract , Indian J. Sci. Technol. 2015;8(17): 63478.
22. Kai Z, Renbo S, Yi G. Corrosion Behavior of Hot-dip Galvanized Advanced High Strength Steel Sheet in a Simulated Marine Atmospheric Environment. Int. J. Electrochem. Sci..2019; 14 : 1488 – 1499.

حماية معدن الكلفانك ستيل من التآكل في الوسط الملحي بوساطة دقائق الكبريت النانوية

احلام محمد فرحان

منى سرحان صندوق

رشا عبد جاسم

قسم الكيمياء، كلية العلوم للبنات، جامعة بغداد، بغداد، العراق

الخلاصة :

تم دراسة خصائص الكبريت النانوي بوساطة جهاز مجهر القوة الذرية. أظهرت قياسات مجهر القوة الذرية الحجم الكلي للكبريت النانوي المحضر بوساطة مزج ثايوسلفات الصوديوم مع مستخلص نبات اليقطين مساويا 93.62 نانومتر. تم دراسة حماية التآكل لمعدن الكلفانك ستيل في الوسط الملحي وبمختلف درجات الحرارة بوساطة الكبريت النانوي وتم الحصول على افضل نتائج ثرموديناميكية للمعدن بوجود الكبريت النانوي حيث كفاءة التثبيط ومقاومة لتآكل للمعدن تعطي اعلى قيمة عند اعلى درجة حرارية بوجود المثبط بلمقارنة بغيابته. كذلك سرعة التآكل تقل عند زيادة درجة الحرارة بوجود الكبريت النانوي، القيم الموجبة للدالة الحرارية بوجود المثبط وبعدم وجود الكبريت النانوي تدل على انه التفاعل ماص للحرارة . لذا يقترح ان الكبريت النانوي مثبط جيد لمعدن الكلفانك ستيل في الوسط الملحي.

الكلمات المفتاحية: مستخلص نبات اليقطين، التآكل، كلفانك ستيل، كبريت النانوي، الدوال الثرموديناميكية، ثايوسلفات صوديوم.